PAPER

Dominant structural defects in amorphous silicon

IOP Publishing Journal of Physics: Condensed Matter
J. Phys.: Condens. Matter **27** (2015) 345004 (9pp) doi:10.1088/0953-8984/27/34/345004

Dominant structural defects in amorphous silicon

Paule Dagenais, Laurent J Lewis and Sjoerd Roorda

Département de Physique et Regroupement Québécois sur les Matériaux de Pointe (RQMP), Université de Montréal, C.P. 6128, Succursale Centre-Ville, Montréal, QC H3C 3J7, Canada

E-mail: laurent.lewis@umontreal.ca

Received 21 May 2015, revised 30 June 2015
Accepted for publication 3 July 2015
Published 3 August 2015

Abstract

The nature of disorder in amorphous silicon (a-Si) is explored by investigating the spatial arrangement and energies of coordination defects in a numerical model. Spatial correlations between structural defects are examined on the basis of a parameter that quantifies the probability for two sites to share a bond. Pentacoordinated atoms are found to be the dominant coordination defects. They show a tendency to cluster, and about 17% of them are linked through three-membered rings. As for tricoordinated sites, they are less numerous, and tend to be distant by at least two bond lengths. Typical local geometries associated to under and overcoordinated atoms are extracted from the model and described using partial bond angle distributions. An estimate of the formation energies of structural defects is provided. Using molecular-dynamics calculations, we simulate the implantation of high-energy atoms in the initial structure in order to study the effect of relaxation on the coordination defects and their environments.

Keywords: amorphous silicon, molecular dynamics, defects

(Some figures may appear in colour only in the online journal)

1. Introduction

Amorphous materials are of considerable importance in condensed-matter science, largely because of their technological interest, and because they raise fundamental questions about the exact nature of disorder in non-crystalline solids [1]. Despite a vast literature pertaining to the structural, electronic and thermodynamic properties of amorphous silicon (a-Si), for example, a topological definition of this covalent semiconductor is still lacking. Of particular interest is the characterization of structural defects since they play a major role in several respects. As for the electronic behavior, electrons are responsible for the states located in the gap and in the band tails of the density of states [2]. They also influence structural properties, causing such a phenomenon as the decrease of the viscosity related to the mobility of dangling bonds—unsatisfied bonds associated with undercoordinated atoms [3, 4]. Since a-Si offers great promises in the field of photovoltaic technologies, the study of structural defects is a step toward understanding the degradation of photo-conversion devices induced by extended exposure to light [5]. Many questions remain regarding the distribution of defects within the system: are they spread evenly or located on small and highly strained regions? Are over or undercoordinated atoms the intrinsic coordination defects in a-Si? Can we associate defects to typical local geometries? We address such questions in the present work.

The identification and characterization of defects in computer models of a-Si has been the object of several investigations [2, 4, 6–11]. Some studies have revealed important similarities between thermal relaxation in amorphous silicon and the recombination of point defects in the crystalline phase. This observation led to the idea that structural defects in a-Si are akin to vacancies and interstitials (Frenkel pairs) [9, 12, 13], which would be introduced in the structure during the amorphization process and which could afterwards be annihilated by annealing. The possibility of identifying vacancies in the damaged structure was demonstrated based on an anomalous relation between the Voronoi volume and the charge of nearby atoms [9]. Other authors have investigated the distributions and local environments of coordination defects in configurations obtained by rapidly cooling from the liquid phase,

using molecular-dynamics (MD) simulations and empirical potentials such as Tersoff [6] or Stillinger–Weber [14]. In both cases, it was found that undercoordinated sites are less numerous than overcoordinated sites; coordination is defined here in terms of nearest-neighbours, themselves defined in terms of a cutoff radius. It was also observed that overcoordinated sites share bonds more than if they were randomly distributed and that they form bonds longer than the average bond length. The model built with the Tersoff potential, further, showed that overcoordinated atoms typically exist in two types of geometries: a nearly spiked configuration (see below), and one attached to a three-membered ring, resulting in a bond angle distribution centered on 90° with a secondary peak at 60°. In this model, all tricoordinated atoms were found to lie in a planar geometry (sp^2 orbitals), which corresponds to a bond angle distribution centered on 120°. With the Stillinger–Weber potential, about 25% of overcoordinated sites were found to belong to three-membered rings, and the other 75% are embedded in nearly-tetrahedral environments, with a fifth bond in the direction opposite to one of the tetrahedral positions. The main peak of the bond angle distribution for three-coordinated defects was measured at ∼105°, with secondary peaks at 90° and 130°.

A corresponding analysis was carried out in a 64 atom model built by relaxing a randomly-packed system using a conjugate-gradient algorithm within an *ab initio* scheme [15, 16]. This study revealed that the mean bond angle for tricoordinated atoms is somewhat smaller than the crystalline value. No planar configurations were found for undercoordinated sites; instead, the topologies associated with a bond angle of 120° were attributed to distorted tetrahedra. This model revealed that pentacoordinated atoms tend to form weaker (longer) bonds, and that usually one of their neighbors is tricoordinated. Depending on the density, the average coordination number in the system is 4.03 (for a density of 2.6 g cm^{-3}) or 3.97 (for a density of 2.3 g cm^{-3}).

It must however be noted that the above studies were based on computer models that are not optimal. The model considered in [15, 16], for example, does not fit closely with experiment—e.g. the first minimum in the radial distribution function (RDF) is much higher than in experiment. On the other hand, models based on rapid cooling from the melt result in frozen-in liquid configurations because the cooling rate is much too large. Thus, these models result in a total bond angle distribution that retains a clear signature of the liquid, viz. secondary peaks at low angles around 60° and 80° [7, 8, 14, 17]. In addition, the width of the distribution is somewhat larger than the experimental value [13] ($\Delta\theta_t \simeq 14$–$16°$ versus $\simeq 10°$). Thus, it is not clear if the predominance of fivefold sites, which results in an average coordination number greater than four, is a consequence of the liquid character remaining in the glassy state or if it is truly representative of the amorphous phase.

Questions regarding the nature of structural defects and the predominance of one over the other remain a matter of debate. Pantelides introduced the notion of floating and dangling bonds, respectively associated with over and undercoordinated sites [18]. Based on theoretical and experimental results, he argued that the main active center in electron paramagnetic resonance (EPR) experiments was the floating bond. Further studies based on EPR measurements however concluded that the dangling bond was the basic structural defect in a-Si [19–21]. In subsequent work using tight-binding calculations, it was shown that only dangling bonds are EPR active whereas floating bonds give rise only to tiny magnetic moments, i.e. overcoordinated atoms would not be detected by EPR experiments [22]. Thus, it is not yet clear what is the dominant intrinsic defect in a-Si.

In this work we examine a realistic model of a-Si initially fabricated with the Wooten, Winer and Weaire (WWW) algorithm [23], and conclude that the dominant structural defect is the pentacoordinated site. The size of the system is particularly important in the study of defects, since these represent only a small percentage of the sites; the model used here consists of 100 000 atoms. We find that tricoordinated atoms are anticorrelated, i.e. prefer not to form bonds with one another, and this is a consequence of thermal relaxation (annealing). In contrast, bonds between overcoordinated atoms are favored, and this tendency is amplified by annealing. Pairs of over/undercoordinated sites have a slight tendency to share bonds, which disappears upon thermal relaxation. Our model provides information about typical atomic geometries of coordination defects. For tricoordinated sites, first neighbors are typically arranged either in a planar geometry or in a deformed tetrahedral structure. Isolated pentacoordinated atoms are also found in tetrahedral-like conformations, with an extra fifth neighbor, or else are disposed in a spiked configuration with three atoms placed in a plane forming bonds of ∼120° and the other two located above and below this plane. About 17% of overcoordinated sites belong to three-membered rings.

2. Theoretical context and methodology

2.1. Computational details

This work is based on a model of amorphous silicon containing 100 000 atoms and produced with an optimized version of the WWW algorithm [23–26], kindly provided by Mousseau. We examine the system in five different states: states A1 and A2 refer to one or two successive annealing cycles of the initial WWW model. State B is obtained by implanting high-energy atoms in the A1 structure, and state C results from subsequent annealing of this system. Details of the structure and state of energy of the model in its different states, as well as a complete description of the numerical simulations, can be found elsewhere [27]. We simply mention here that all simulations were carried out using the Stillinger–Weber interatomic potential (using the set of parameters fitted to the amorphous phase [28]) within the MD package LAMMPS [29].

2.2. Connectivity of the amorphous structure

The definition of atomic bonds—and hence first-neighbors—in disordered systems is ambiguous, in particular in empirical models where information about the electronic density is not available. The simplest way to define first neighbors is in

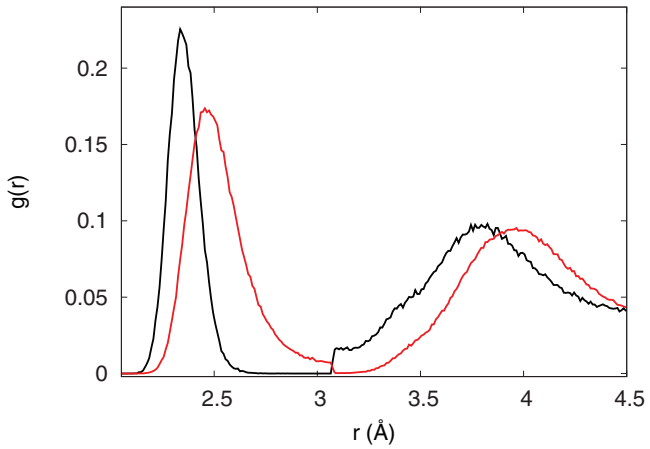

Figure 1. Discontinuities at $r = r_c = 3.075$ Å in the partial RDFs $g_{34}(r)$ (black) and $g_{54}(r)$ (red)—see text for details.

terms of a cutoff radius (r_c), which is located in the minimum following the first peak of the RDF. Since this minimum is non-zero, the connectivity of the system, and thereby the identification and character of coordination defects, depend on the choice of r_c. As will be discussed below, a parameter used to probe spatial correlations between defect types may be constructed from partial RDFs $g_{ij}(r)$ which give the probability (per unit volume) to find a j-coordinated atom at a distance r from an i-coordinated atom. The weighted sum of the partial RDFs gives the total RDF $g(r)$:

$$g(r) = \sum_{i,j} g_{ij}(r) \times \frac{N_i}{N_{\text{tot}}} \tag{1}$$

where N_i is the total number of i-coordinated atoms. Because there is a continuum of atoms in the (non-zero) first minimum of the total RDF, some of the partial RDFs change discontinuously at $r = r_c$ (here $r_c = 3.075$ Å—see below). For example, for a pentacoordinated site, the probability of finding a first neighbor falls to zero discontinuously at a radial distance equal to the cutoff radius, since it is $r = r_c$ which determines whether an atom is a first neighbour or not. On the other hand, for a tricoordinated site, the probability of finding a second neighbor goes discontinuously from zero to a non-zero value at $r = r_c$, since it is this value that defines the minimal distance at which other atoms are considered second neighbors. As a result, $g_{34}(r)$ rises discontinuously at $r = r_c$. Those two features are illustrated in figure 1, where $g_{34}(r)$ and $g_{54}(r)$ are shown.

In a study based on the local density approximation within density functional theory, Stich *et al*. introduced the notion of weak bonds [17], a type of defect different from those mentioned earlier. In terms of electronic density, such a bond is characterized by two low maxima instead of a single maximum centered on the bond as is the case for normal tetracoordinated atoms. Geometrically, we may define a weak bond as a bond whose length is somewhat larger than the average bond length, thus in some interval in between the first and second peaks in the RDF. There is no absolute way to define this interval because the RDF is nowhere zero in this region, and because the first and second-neighbour peaks have a significant width and are not symmetric. However, a visual inspection of the RDF reveals that the second-neighbor peak starts at about 3.075 Å, and this is the value we have used for r_c (unless otherwise noted), which includes long bonds, while the first-neighbor peak dies at about 2.935 Å, and this is the lower bound we have used for defining weak bonds. Thus, according to this definition, weak bonds are included in the connectivity table when $r_c = 3.075$ Å, but excluded if $r_c = 2.935$ Å.

That being said, three-coordinated defects do not seem to admit weak bonds since moving r_c from left to right in the r_c interval does not yield new three-coordinated neighbors in the connectivity table. In contrast, some pentacoordinated sites do form weak bonds upon changing r_c. A subset of overcoordinated atoms that do not possess weak bonds can thus be identified, and these will be used below to characterize the local environments of defects.

Despite the fact that the upper value of the r_c interval (3.075 Å) seems like a more natural choice for r_c based on the concept of weak bonds, it remains to some degree arbitrary. Variables such as the number of i-coordinated defects or the correlation parameter P_{ij} (which will be introduced in the next section) may vary quantitatively depending on r_c; however, the tendencies that we observe, for example the increase or decrease of those quantities as a response to implantation or annealing, were verified not to be affected by the inclusion or exclusion of weak bonds, and it is those tendencies that we intend to identify in this work.

2.3. The spatial correlation parameter

Similarly to the analysis by Ishimaru of a melt-and-quench a-Si model [6], we introduce a parameter (P_{ij}) which probes spatial correlations between atoms according to their coordination number. It allows to determine if coordination defects are randomly distributed in the amorphous system or if, rather, they are spatially correlated (tendency to form bonds) or anti-correlated (tendency not to form bonds). P_{ij} is defined in terms of Z_{ij}, the average number of j-coordinated neighbors of an i-coordinated atom, which itself is computed from the partial RDF $g_{ij}(r)$:

$$Z_{ij} = \int_0^{r_c} 4\pi r^2 \rho_0 g_{ij}(r) \mathrm{d}r \tag{2}$$

$$P_{ij} = \frac{Z_{ij}}{\sum_k Z_{ik}} = \frac{Z_{ij}}{i}, \tag{3}$$

where the index k covers all possible coordination numbers.

For the purpose of comparison, we define a reference parameter P_{ij}^{ref} that corresponds to a network in which atoms and bonds are randomly distributed so that the position and the coordination number of an atom are two uncorrelated variables. It is defined as follows. Each bond supports two ends; let E_i be the number of bond ends (in the whole system) attached to an i-coordinated atom and L_{ij} the probability for a bond to possess an i-type end and a j-type end. We can thus write:

$$P_{ij} = \frac{L_{ij}}{\sum_k L_{ik}}. \quad (4)$$

In a totally random system we have:

$$L_{ij}^{\text{ref}} = \frac{E_i \times (E_j - j\delta_{ij})}{\left(\sum_k E_k\right)^2} = \frac{\mathrm{i}N_i \times j(N_j - \delta_{ij})}{\left(\sum_k kN_k\right)^2} \quad (5)$$

so that

$$P_{ij}^{\text{ref}} = \frac{j(N_j - \delta_{ij})}{\sum_k k(N_k - \delta_{ik})}. \quad (6)$$

Spatial correlations between coordination defects can thus be evaluated by comparing P_{ij} in the amorphous system with the reference P_{ij}^{ref}. A ratio of 1 indicates a complete absence of correlations between the coordination number of an atom and those of its neighbors; a ratio of x indicates that the probability for a neighbor of an i-coordinated site to be j-coordinated (both chosen randomly in the amorphous system) is x times higher than in a system with sites and bonds distributed randomly. This ratio is symmetric with respect to the i and j indices, since the probability L_{ij} is itself symmetric.

3. Results and discussion

3.1. Spatial correlations between coordination defects

Four statistically independent simulations were performed, simply by changing the seed of the random number generator used to set the initial temperature of each annealing cycle. This provides a confidence interval on the correlation parameters and the number of coordination defects. We note that, while the results vary a bit from run to run, the tendencies shown by the different runs are the same. For each of the four simulations, the results were averaged over 25 configurations, for a total of 100 configurations; this is necessary in order to have proper statistics for defects which are less abundant. The results are presented in table 1.

We examine first the model in state A1 (i.e. after one annealing cycle). It contains 2.1% of overcoordinated atoms and 0.89% of undercoordinated atoms; we will return to this observation below when we discuss the energetics of defects. Another interesting observation is the fact that overcoordinated sites tend to be connected within three-membered rings (see right panel of figure 2): in state A1, ∼17% of these sites are found in triangular geometries, compared to ∼22% in state B, and ∼17% in state C; moreover, ∼77% of three-membered rings contain only pentacoordinated sites. The predominance of pentacoordinated sites may seem at odds with experiment—x-ray diffraction measurements indicate that the average coordination number is 3.79 in the as-made sample and raises to 3.88 after annealing [13], which suggests a majority of undercoordinated sites. In our model, the corresponding values are 4.017 and 4.013 (see states B and C in table 1). The exact values evidently depend on the particular choice of r_c. However, a most important factor is the way coordination numbers are calculated in experiment. Indeed, they are obtained by fitting a Gaussian curve to the first peak of the RDF, which can then be integrated; the distribution of nearest–neighbors is thus assumed to be symmetric. In our model, the first peak of the RDF does not resemble a Gaussian: the right-hand side extends more than the left-hand side, leading to larger coordination numbers. If we proceed as in experiment (but fit the Gaussian to the left-hand side and multiply by two), we find the coordination number to increase from 3.26 in state B to 3.30 in state C. These numbers cannot be compared directly to experiment; however, this demonstrates that the model behaves the same as in experiment—the coordination number approaches 4 upon annealing.

Table 1. Distribution of coordination defects in the a-Si model in four different states (see section 2.1).

	A1	A2	B	C
N_2	0	0	2	1
N_3	886	844	974	875
N_4	96 995	96 983	96 437	96 936
N_5	2112	2165	2572	2182
N_6	7	8	16	7
$\langle Z \rangle$	4.013	4.013	4.017	4.013
$P_{33}/P_{33}^{\text{ref}}$	0.284	0.225	0.449	0.279
$P_{35}/P_{35}^{\text{ref}}$	1.34	1.13	1.33	1.21
$P_{55}/P_{55}^{\text{ref}}$	3.76	4.15	4.32	3.84

Table 1 shows that threefold sites are anti-correlated ($P_{33}/P_{33}^{\text{ref}} < 1$), i.e. they tend to be separated by at least two bonds. In contrast, fivefold sites are positively correlated, with $P_{55}/P_{55}^{\text{ref}} = 3.76$ (in state A1 as an example). Thus, if we randomly select a 5-coordinated site, and pick one of its first neighbors, the probability for it to be also 5-coordinated is 3.76 higher than if the system was totally random.

These results are presented in a more visual manner in figure 2 where we show undercoordinated atoms only in the left panel and overcoordinated atoms only in the right panel, for model A1. Pentacoordinated defects show an interesting tendency to form three-membered rings. In fact, ∼77% of three-membered rings are composed only of overcoordinated atoms. We find similar results upon relaxing our model with other potentials, viz. EDIP [8] and Tersoff [30]. The presence of three-membered rings may therefore be viewed as a signature of the presence of penta-coordinated atoms; we will return to this point below.

The implantation of energetic atoms leads to the creation of new coordination defects, of all types (see table 1, column B). The process reduces the anticorrelated character of undercoordinated atoms, as $P_{33}/P_{33}^{\text{ref}}$ increases slightly while remaining smaller than 1. This is due to the fact that the trajectories of implanted atoms result in highly-strained regions in which the newly-created defects are confined. Subsequent to annealing, $P_{33}/P_{33}^{\text{ref}}$ returns to a value comparable to that in the initial system (state A1). Also, a second annealing cycle decreases slightly the correlation parameter for undercoordinated sites: $P_{33}/P_{33}^{\text{ref}}$ goes from 0.284 to 0.225 between states A1 and A2.

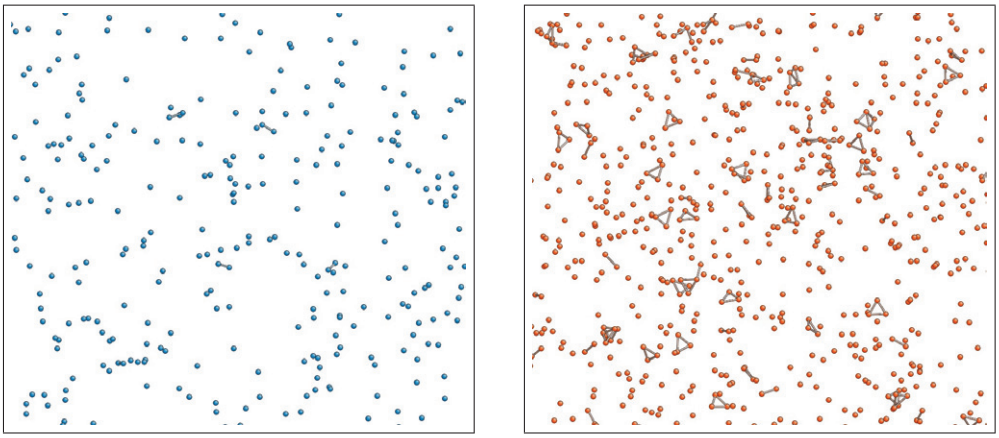

Figure 2. Portions of the a-Si model in state A1. Only 3-coordinated (blue, left) and 5-coordinated (orange, right) atoms are shown. Undercoordinated sites show a tendency to be separated by at least two bonds, whereas overcoordinated sites tend to attract one another.

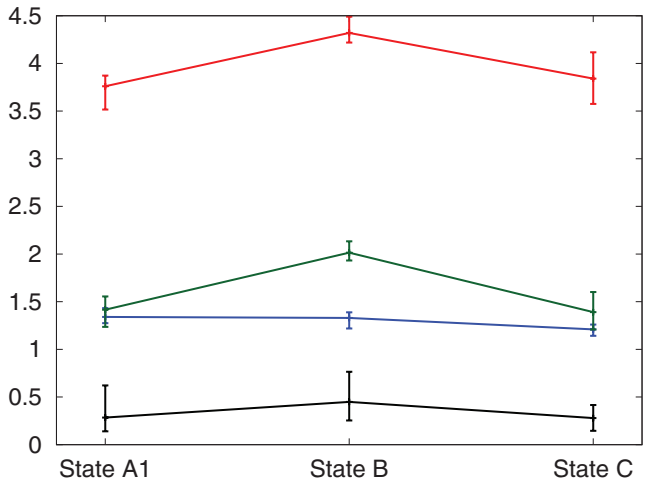

Figure 3. Correlations between coordination defects during implantation and annealing. Black line: $P_{33}/P_{33}^{\mathrm{ref}}$; blue line: $P_{35}/P_{35}^{\mathrm{ref}}$; green line: $P_{55}/P_{55}^{\mathrm{ref}}$ excluding weak bonds; red line: $P_{55}/P_{55}^{\mathrm{ref}}$ including weak bonds. The 'error bars' indicate the range of values from the four statistically independent simulations.

We conclude that structural relaxation favors the anticorrelation of tricoordinated sites.

Likewise, $P_{55}/P_{55}^{\mathrm{ref}}$ increases slightly upon implantation—here again because of the confinement of defects in the implantated zone—, from 3.76 (A1) to 4.32 (B). When the implanted system is thermally relaxed (state C), $P_{55}/P_{55}^{\mathrm{ref}}$ returns to 3.84, a value comparable to that in the non-implanted model (A1). The values of $P_{55}/P_{55}^{\mathrm{ref}}$ corresponding to systems A1, B and C (extracted from a single simulation) are shown in figure 3, including or excluding weak bonds in the connectivity (red and green curves, respectively). The inclusion of weak bonds causes $P_{55}/P_{55}^{\mathrm{ref}}$ to shift upwards and does not affect its general aspect; we conclude, therefore, that the changes induced by implantation and annealing occur through normal bonds, not weak bonds. The spatial correlation between overcoordinated sites increases with thermal relaxation, since $P_{55}/P_{55}^{\mathrm{ref}}$ goes from 3.76 to 4.15 between first and second annealing (A1 and A2).

The value of $P_{35}/P_{35}^{\mathrm{ref}}$ is slightly larger than 1, i.e. the spatial correlation between under and overcoordinated atoms is barely stronger than in the random reference system. It is little affected by implantation and approaches one with thermal relaxation so that correlations disappear with sufficient annealing. Hence, 3 and 5-coordinated defects that subsist in states A2 and C are more isolated from each other than in state A1. This effect presumably originates from a series of bond recombinations for neighboring pairs of under/overcoordinated sites.

3.2. Local environment of structural defects

3.2.1. Interatomic distances. Different structural defects correspond to different local geometries. Figure 4 presents the distributions of first-neighbor distances for three, four and five-coordinated sites in sample A1. The mean bond length is 2.398 Å averaged over all atoms, and it is 2.323 Å, 2.349 Å and 2.454 Å for three, four and five-coordinated atoms, respectively, with corresponding variances of 0.087, 0.091, and 0.18. Thus, tricoordinated sites tend to form shorter bonds, whereas pentacoordinated atoms form longer (weak) bonds, with a much wider bond length distribution, indicating that these defects belong to a larger variety of local environments.

3.2.2. Tetrahedral angles. Figure 5 displays the partial bond angle distributions for under and overcoordinated atoms, from which we can extract some information about the local geometries of the defects. First, these distributions verify the point that pentacoordinated sites belong to a wider range of conformations than tricoordinated sites, since the variances of the partial distributions for over and undercoordinated atoms are, respectively, 24.57° and 10.09°. For bond angles associated with tricoordinated sites, the distribution is centered about 112.9°. It was shown above that these defects mostly have neighbors which are tetracoordinated. As will be discussed in section 3.2.4, tricoordinated sites occur mainly in two types of geometries : a distorted tetrahedral conformation, which favors bond angles around the crystalline value (109.5°), and a planar conformation, which results in bond angles around 120°.

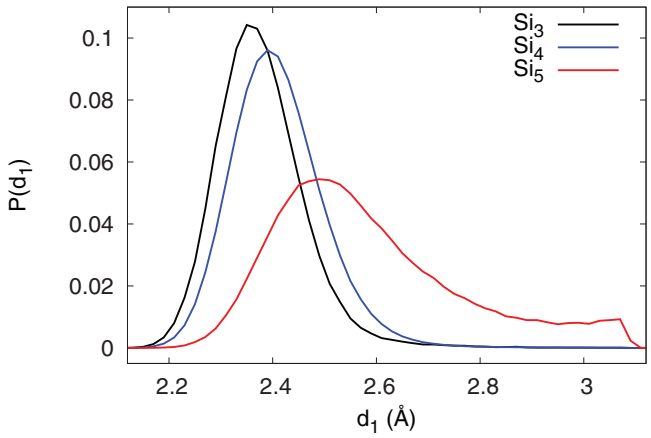

Figure 4. Distributions of first-neighbor distances for three (black), four (blue) and five-coordinated (red) atoms.

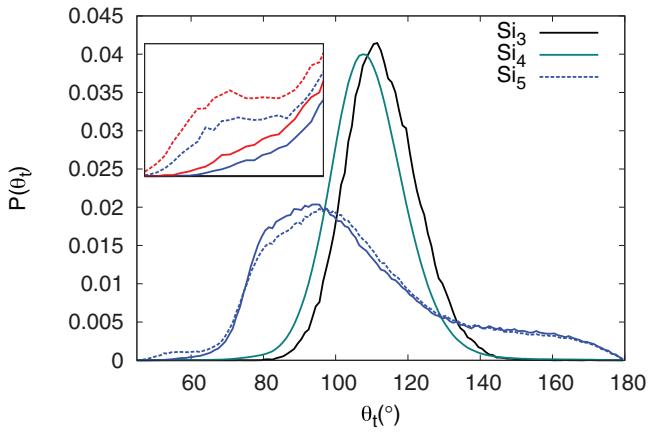

Figure 5. Bond angle distributions for tretracoordinated (green line), undercoordinated (black line) and overcoordinated atoms in sample A1, including or not weak bonds in the connectivity (dashed blue line and solid blue line, respectively). The inset focuses on the small bump around 55° in the distributions for pentacoordinated atoms; we also show in the inset the results for sample B (dashed red line and solid red line).

The blue curves in figure 5 correspond to angles centered on 5-coordinated sites, including or not weak bonds in the connectivity map (dashed and solid line, respectively). Bond angle distributions extracted from melt-and-quench a-Si models (using either the Tersoff potential [7], EDIP [8], or *ab initio* calculations [17]) suggest a similarity between the local environments of overcoordinated atoms in our model and in the liquid phase of silicon. In those models, the bond angle distribution of the liquid phase is characterized by a large main peak centered on 100°, in addition to a secondary peak at 60°; upon cooling into the amorphous state, the main peak narrows down and moves toward the crystalline value while the amplitude of the secondary peak becomes very small. For angles subtended by overcoordinated atoms in our model, the main peak is centered on 90° and the distribution remains non negligible up to a very high value (∼170°). The low secondary peak is near 55° (see figure 5) and arises from the inclusion of weak bonds in the distribution (dashed blue line). Since bond angles around 60° are associated with triangular geometries, this suggests that overcoordinated atoms forming triangular geometries are linked through weak bonds. In fact, the proportion of pentacoordinated sites linked in three-membered rings is very sensitive to the inclusion of weak bonds in the connectivity: if these are excluded (by setting the radial cutoff at 2.935 Å), this proportion in model A1 is only ∼3%, but it rises to ∼17% if weak bonds are included (by setting the cutoff to 3.075 Å). The red curves in the inset of figure 5 correspond to the partial distributions of the as-implanted system (state B). Again, the dashed line includes weak bonds and the solid line excludes them. Implantation causes a small decrease of the main peak, and a slight increase around 55°, which disappears upon annealing. This indicates that the number of triangular conformations has grown as a response to implantation. As mentioned in section 3.1, in the initial, as-implanted and annealed states (A1, B and C), the portion of overcoordinated sites forming three-membered rings is respectively ∼17%, ∼22% and ∼17%.

3.2.3. Formation energies of structural defects. The local environments of structural defects can also be characterized by the distributions of potential energies for the defects themselves and their first-neighbor shells. The distributions of potential energies for the different atom types (in state A1) are characterized in table 2 in terms of mean values and standard deviations (in parentheses). These distributions are also illustrated in figures 6 and 7. Despite the fact that the distributions have significant widths, they clearly demonstrate that defective atoms are not equivalent in terms of their energetic properties. Four independent simulations were performed to anneal the initial configuration into state A1 ; it was found that per-atom energies (from the Stillinger–Weber potential) do not vary more than 0.16% from run to run. The first column of table 2 displays the mean potential energies for different types of atoms; the average for all atoms (E_{ave}) is −3.016 eV at^{-1}. Evidently, these energies do not necessarily reflect the predominance of certain types of atoms since the local environments must also be taken into account for this purpose. The second column presents the energies of those nearest–neighbors which are tetracoordinated. To evaluate the energy cost of a defect, we average the potential energy of the defect itself and its nearest–neighbors, and take the difference with the energy of tetracoordinated sites with no defective neighbors. Doing so we find 0.171 eV at^{-1} for threefold atoms, 0.120 eV at^{-1} for isolated fivefold atoms and 0.076 eV at^{-1} for overcoordinated atoms within three-membered rings. These numbers explain why overcoordinated atoms are more numerous (2.1% versus 0.89%), and why such a high proportion of them (∼17% in state A1) tend to form three-membered rings ; this proportion is stable under successive annealings. The fact that the energy cost is higher for tricoordinated sites than for pentacoordinated sites is in line with calculations reported in [6], where the formation energies are found to be 0.45 and 0.3 eV, respectively; while the absolute values are different from our values, because models and potentials are different, the differences are quite similar (0.45–0.30 versus 0.171–0.076).

It is interesting to examine how the energy cost is shared between the defects and their environments. For this purpose, we examine the mean potential energies of different types of

Table 2. Mean potential energy of different types of atoms. The global average for the system in state A1 is $E_{ave} = -3.016$ eV at^{-1} (0.132 eV).

Type of atom	E (eV/at.)	1st neighbors' E (eV/at.)
Si_4	− 3.035 (0.094)	—
Si_3	− 2.316 (0.094)	− 3.048 (0.167)[a]
Si_5	− 3.080 (0.180)	− 2.878 (0.184)[a]
Si_5 △	− 2.853 (0.192)	− 2.994 (0.102)[a]
Si_5 no-△	− 3.128 (0.403)	− 2.871 (0.172)[a]

Si_4: tetracoordinated atom with no defective neighbors
Si_3: tricoordinated atom
Si_5: pentacoordinated atom
Si_5 △: pentacoordinated atom belonging to a triangular geometry[b]
Si_5 no-△: pentacoordinated atom not belonging to a triangular geometry[b]
[a]Only tetracoordinated atoms
[b]Triangular geometry refers to a three-membered ring formed of 5-coordinated atoms only
Note: The values in parentheses are the standard deviations.

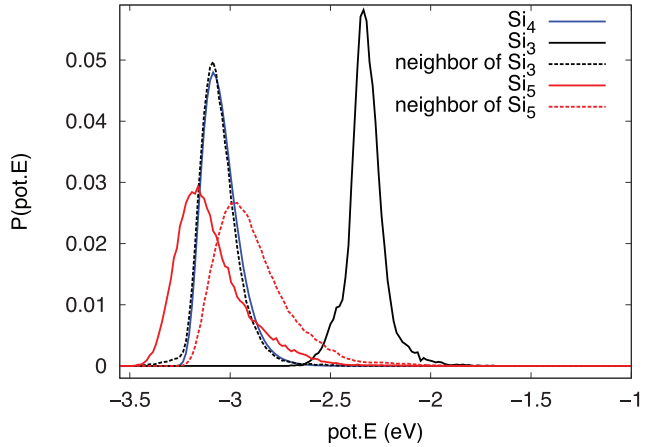

Figure 6. Distributions of potential energies for tetracoordinated (Si_4), tricoordinated (Si_3), and pentacoordinated (Si_5) atoms, as well as their first neighbors; the labels refer to those of table 2.

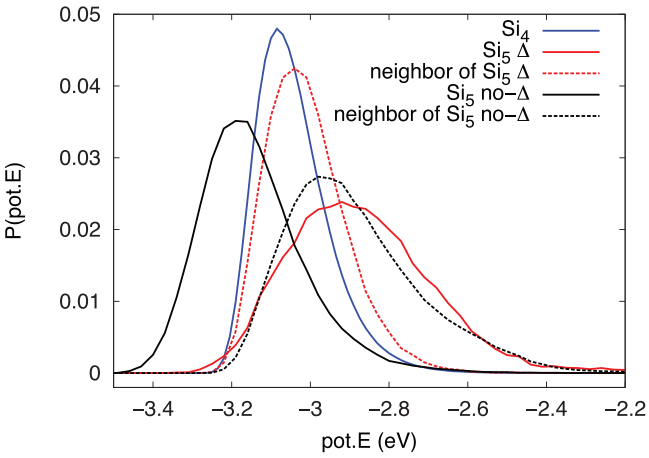

Figure 7. Distributions of potential energies for tetracoordinated atoms (Si_4), isolated pentacoordinated sites (Si_5 no-△), and pentacoordinated sites belonging to triangular geometries (Si_5 △), and for their first neighbors; the labels refer to those of table 2.

defects, and compare them with the energy of tetracoordinated atoms, which we use as a reference ($E = -3.035$ eV). Undercoordinated defects have a potential energy higher than the energy of non defective sites ($\Delta E = 0.719$ eV at^{-1}), while their first neighbors are almost at par with the reference value ($\Delta E = -0.013$ eV at^{-1}). Thus, essentially all of the excess energy in an undercoordinated defect lies in the defect itself. This can also be inferred from figure 6, since the distribution of potential energies for first neighbors of tricoordinated atoms fits with that for non-defective sites. As for overcoordinated atoms, two cases may be distinguished. Pentacoordinated defects arranged in three-membered rings absorb the bulk of the energy cost ($\Delta E = 0.182$ eV at^{-1}), while neighboring tetracoordinated atoms are close to the reference value ($\Delta E = 0.041$ eV at^{-1}). In contrast, isolated overcoordinated sites have potential energies below the reference value ($\Delta E = -0.093$ eV at^{-1}) while neighbouring tetracoordinated sites lie higher in energy ($\Delta E = 0.164$ eV at^{-1}). We note that the distribution of potential energies for pentacoordinated atoms belonging to triangular geometries and the distribution for first neighbors of pentacoordinated sites *not* belonging to such geometries are very similar (see the curves labelled *Si_5*△ and *neighbors of Si_5 no-*△ in figure 7). This indicates that if a 5-coordinated defect does not belong to a triangular conformation, it is very likely that one if its neighbors does; this feature can be interpreted as a manifestation of the spatial correlation between overcoordinated sites. Finally, if we compare the distribution for all pentacoordinated atoms (*Si_5* in figure 6) with the distribution for pentacoordinated atoms not belonging to triangular geometries (*Si_5 no-*△ in figure 7), we find that they are also very similar, but this is to be expected since a majority of 5-coordinated sites are not linked in three-membered rings (in state A1, only ∼17% are).

3.2.4. Typical conformations for coordination defects. Tricoordinated defects are mostly found in two types of geometries. The first one resembles a distorted tetrahedral configuration, as illustrated on the left panel of figure 8. Conformations shown in figure 8 (and similar figures below) were extracted directly from the model in state A1, i.e. they correspond to real atomic positions in the system; it is therefore possible to calculate the potential energies of those specific atoms. The tetrahedral geometry shown in figure 8 suggests the presence of a fourth atom (not bonded to the central atom according to our connectivity table), in a direction perpendicular to the plane formed by atoms 2, 3 and 4. It corresponds to the canonical geometry of primitive lattice defects in c-Si that Pantelides suggested as a possible candidate for primitive defects in a-Si [18]. The second geometry is planar, corresponding to sp^2 orbitals, and is shown on the right panel of figure 8. In the *melt and quench* configuration studied in [6], undercoordinated sites strictly appear in planar geometries, resulting in a bond angle distribution centered on 120°. For the deformed tetrahedral and the planar geometries illustrated in figure 8, the potential energies of the defects are, respectively, −2.260 eV and −2.265 eV, which is about 0.773 eV over the potential energy of a non defective site; this value is in agreement with the global average presented in table 2.

Figure 9 shows two types of geometries associated with isolated overcoordinated atoms. When Pantelides first

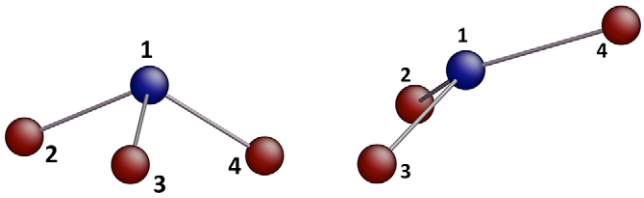

Figure 8. Typical configurations for undercoordinated atoms: deformed tetrahedral geometry (left) and planar geometry (right).

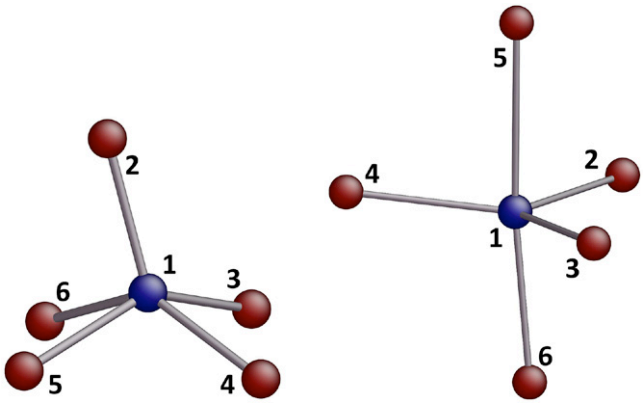

Figure 9. Typical environments for overcoordinated atoms: deformed tetrahedral geometry (left) and spiked conformation (right).

introduced the notion of floating bonds, he inferred that the conformation made of four atoms in tetrahedral positions, with a fifth bond across from one of those directions, should be the canonical configuration for primitive defects in a-Si, as in c-Si [18]. The large variability of bond lengths and bond angles in the amorphous structure allows to associate the two geometries shown in figure 9 with this canonical conformation. On the left, four atoms are positioned in a plane while the fifth bond is approximately perpendicular to this plane. On the right panel of figure 9, the conformation comprises two colinear bonds intersected by a plane containing the three others. The potential energies of the central defects, for those two geometries, are respectively −3.099 eV and −3.183 eV, i.e. 0.064 eV and 0.148 below the energy of a tetracoordinated site. This is consistent with the fact that it is the environment which absorbs the bulk of the energy cost, as was discussed in section 3.2.3. The nearly spiked geometry presented on the right panel of figure 9 was also observed in the model studied in [6], where the bond angle distribution was centered on 90°. The author also inferred from that distribution that pentacoordinated sites were attached to three-membered rings, based on a lump around 60°. Figure 10 displays a group of three overcoordinated atoms in a triangular geometry, whose average energy is larger than the energy of a non defective site by 0.197 eV per atom, which compares well with the difference calculated with the average from table 2 ($\Delta E = 0.182$ eV). Triangular structures made of 5-coordinated sites are frequently surrounded by four-membered rings, as is the case here, which generates angles around 90°. As discussed above, this type of conformation is stable under thermal relaxation.

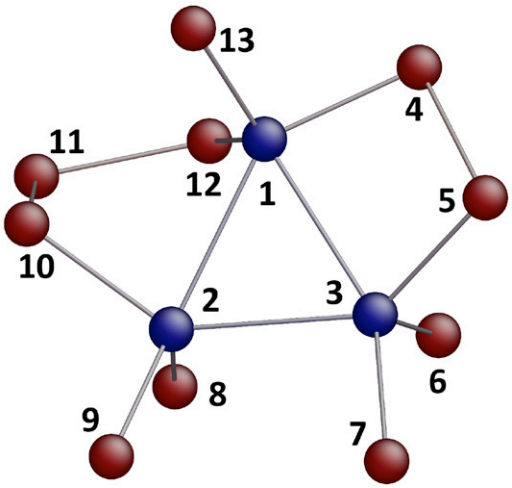

Figure 10. Example of a triangular geometry for overcoordinated atoms; atoms 1, 2 and 3 are connected by weak bonds of lengths $r_{12} = 2.919$ Å, $r_{23} = 2.859$ Å, and $r_{34} = 2.929$ Å.

4. Summary

Several studies have addressed the question of the spatial arrangement of defects in amorphous silicon on the basis of models generated on the computer. Some of these models were obtained using the melt-and-quench technique, others by relaxing a random system with a conjugate-gradient algorithm. Using a modified version of the WWW algorithm, Barkema and Mousseau have fabricated a realistic structural model containing 100 000 atoms [24]. We have characterized the coordination defects in this model in terms of spatial arrangements and surrounding geometries, and this provides a reliable description of the structure at the atomistic level.

We have shown that undercoordinated atoms display a negative spatial correlation, i.e. they prefer not to be nearest neighbors to each other and be separated by at least two bonds; this tendency increases upon annealing. The dominant coordination defects in the model are pentacoordinated sites, as they are energetically more favorable. These are characterized by a positive spatial correlation, i.e. they tend to form bonds. This correlation also increases under the effect of relaxation. Among overcoordinated sites, ∼17% are linked in three-membered rings. This proportion increases slightly upon implantation of high-energy atoms, and returns to a comparable value after annealing. Pairs of neighboring over/undercoordinated defects are a bit more probable than in a totally random system. Nevertheless, thermal relaxation decreases the value of $P_{35}/P_{35}^{\mathrm{ref}}$, which suggests the recombination of dangling and floating bonds.

From the partial distributions of bond angles and bond lengths, we have extracted a description of the local environment of coordination defects. For tricoordinated sites, two typical conformations are observed, one planar and the other resembling a distorted tetrahedron; this causes an average bond angle slightly above the crystalline value. In both cases, the potential energy of defective atoms lies above the system average, whereas first neighbors have energy slightly under the average.

Pentacoordinated sites are predominantly found in three types of geometries, two of which consist of an isolated defect having only tetracoordinated neighbors, while the third one is composed of three interconnected defects, often surrounded by four-membered rings formed of tetracoordinated sites. We have shown that the latter are stable under thermal relaxation. In the case of an isolated pentacoordinated site, the energy cost is absorbed by the first-neighbor shell, and the defect possesses a lower energy than the global average. In contrast, when overcoordinated atoms are bonded in three-membered rings, the energy cost is mostly absorbed by the defect themselves. The energy of their nearest neighbors also lies slightly above the average.

Taking into account the first neighbor shell, the average formation energies for an isolated tricoordinated site, an isolated pentacoordinated site and a triangular conformation made of pentacoordinated atoms are, respectively, 0.171 eV at^{-1}, 0.120 eV at^{-1} and 0.076 eV at^{-1}.

The characterization of coordination defects in a-Si is one step toward defining the nature of disorder in this material. More extensive studies are necessary to achieve a complete description of the atomistic structure of tetravalent amorphous semiconductors. For example, once it is clear how atoms are arranged in the vicinity of coordination defects, an interesting avenue would be to determine how the different local conformations affect the electronic density of states. Besides, *ab initio* calculations could be employed to test the stability of these conformations in the amorphous structure, which would add a validity criterion to the results presented in this paper. First principle calculations could also push further the attempt to define and identify vacancies and interstitials in amorphous materials. Finally, further experiments are needed to identify with certainty the dominant structural defect in amorphous silicon.

Acknowledgments

We are grateful to N Mousseau for providing the coordinates of the initial a-Si model. This work has been supported by grants from the Natural Sciences and Engineering Research Council of Canada (NSERC) and the Fonds de Recherche du Québec—Nature et Technologies (FRQ-NT). We are indebted to Calcul Québec and Calcul Canada for generous allocations of computer resources.

References

[1] Zallen R 1998 *The Physics of Amorphous Solids* (New York: Wiley)
[2] Biswas R, Wang C Z, Chan C T, Ho K M and Soukoulis C M 1989 *Phys. Rev. Lett.* **63** 1491
[3] Witvrouw A and Spaepen F 1993 *J. Appl. Phys.* **74** 7154
[4] Joly J F 2013 Étude sur la cinétique des défauts structuraux dans le silicium amorphe *PhD Thesis* Université de Montréal
[5] Fehr M, Schnegg A, Rech B, Astakhov O, Finger F, Bittl R, Teutloff C and Lips K 2014 *Phys. Rev. Lett.* **112** 066403
[6] Ishimaru M 2001 *J. Phys.: Condens. Matter* **13** 4181
[7] Ishimaru M, Munetoh S and Motooka T 1997 *Phys. Rev.* B **56** 15133
[8] Justo J F, Bazant M Z, Kaxiras E, Bulatov V V and Yip S 1998 *Phys. Rev.* B **58** 2539
[9] Urli X, Dias C L, Lewis L J and Roorda S 2008 *Phys. Rev.* B **77** 155204
[10] Lutz R 1993 Étude de la relaxation des défauts ponctuels dans les matériaux amorphes par dynamique moléculaire *Master's Thesis* Université de Montréal
[11] Pothier J C, Schiettekatte F and Lewis L J 2011 *Phys. Rev.* B **83** 235206
[12] Dias C L 2001 Influence des défauts ponctuels sur la relaxation du silicium amorphe *Master's Thesis* Université de Montréal
[13] Laaziri K, Kycia S, Roorda S, Chicoine M, Robertson J L, Wang J and Moss S C 1999 *Phys. Rev.* B **60** 13520
[14] Stillinger F H and Weber T A 1985 *Phys. Rev.* B **31** 5262
[15] Clark S 1994 Complex structures in tetrahedrally bonded semiconductors *PhD Thesis* University of Durham
[16] Clark S J, Crain J and Ackland G J 1997 *Phys. Rev.* B **55** 14059
[17] Stich I, Car R and Parrinello M 1991 *Phys. Rev.* B **44** 11092
[18] Pantelides S T 1986 *Phys. Rev. Lett.* **57** 2979
[19] Stutzmann M and Biegelsen D K 1988 *Phys. Rev. Lett.* **60** 1682
[20] Phillips J C 1987 *Phys. Rev. Lett.* **58** 2824
[21] Fedders P A and Carlsson A E 1988 *Phys. Rev.* B **37** 8506
[22] Knief S and von Niessen W 1999 *Phys. Rev.* B **60** 5412
[23] Wooten F, Winer K and Weaire D 1985 *Phys. Rev. Lett.* **54** 1392
[24] Barkema G T and Mousseau N 2000 *Phys. Rev.* B **62** 4985
[25] Vink R L C, Barkema G T, Stijnman M A and Bisseling R H 2001 *Phys. Rev.* B **64** 245214
[26] Vink R L C and Barkema G T 2003 *Phys. Rev.* B **67** 245201
[27] Dagenais P *et al* 2015 *J. Phys.: Condens. Matter* **27** 295801
[28] Vink R, Barkema G, van der Weg W and Mousseau N 2001 *J. Non-Cryst. Solids* **282** 248
[29] Plimpton S 1995 *J. Comput. Phys.* **117** 1
[30] Tersoff J 1988 *Phys. Rev.* B **38** 9902